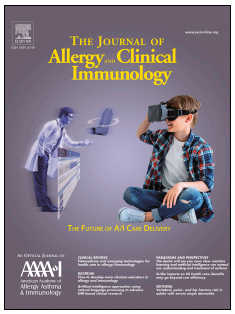
Journal Pre-proof



Structure-guided design of ultrapotent disruptive IgE inhibitors to rapidly terminate acute allergic reactions

Luke F. Pennington, PhD, Pascal Gasser, PhD, Daniel Brigger, PhD, Pascal Guntern, MSc, Alexander Eggel, PhD, Theodore S. Jardetzky, PhD

PII: S0091-6749(21)00730-2

DOI: https://doi.org/10.1016/j.jaci.2021.03.050

Reference: YMAI 15105

To appear in: *Journal of Allergy and Clinical Immunology*

Received Date: 23 September 2020

Revised Date: 24 February 2021

Accepted Date: 26 March 2021

Please cite this article as: Pennington LF, Gasser P, Brigger D, Guntern P, Eggel A, Jardetzky TS, Structure-guided design of ultrapotent disruptive IgE inhibitors to rapidly terminate acute allergic reactions, *Journal of Allergy and Clinical Immunology* (2021), doi: https://doi.org/10.1016/j.jaci.2021.03.050.

This is a PDF file of an article that has undergone enhancements after acceptance, such as the addition of a cover page and metadata, and formatting for readability, but it is not yet the definitive version of record. This version will undergo additional copyediting, typesetting and review before it is published in its final form, but we are providing this version to give early visibility of the article. Please note that, during the production process, errors may be discovered which could affect the content, and all legal disclaimers that apply to the journal pertain.

© 2021 Published by Elsevier Inc. on behalf of the American Academy of Allergy, Asthma & Immunology.

Journal Pre-proof

Title:

Structure-guided design of ultrapotent disruptive IgE inhibitors to rapidly terminate acute allergic reactions

Authors: Luke F.Pennington, PhD[1,2,3,6], Pascal Gasser, PhD[4,5,6], Daniel Brigger, PhD[4,5], Pascal Guntern, MSc[4,5], Alexander Eggel, PhD[4,5]* & Theodore S. Jardetzky, PhD[1,2,3]*

Affiliations:

[1]Department of Structural Biology, Stanford University School of Medicine, Stanford California 94305.

[2]Progam in Immunology, Stanford University School of Medicine, Stanford California 94305.

[3]Sean N. Parker Center for Allergy Research at Stanford University.

[4]Department of Rheumatology and Immunology, Bern University Hospital, Switzerland.

[5]Department of BioMedical Research, University of Bern, Switzerland.

[6]These authors contributed equally.

*These authors jointly supervised this work.

Corresponding authors: Alexander Eggel, Department of BioMedical Research, University of Bern, Bern, Switzerland. Theodore S. Jardetzky, Department of Structural Biology, Stanford University School of Medicine, Stanford, USA. E-mail: alexander.eggel@dbmr.unibe.ch or tjardetzky@stanford.edu.

Disclosure of potential conflict of interest: LF, AE and TSJ are co-founders and shareholders of Excellergy, a company developing new therapeutic modalities in various diseases. All other authors declare that they have no relevant conflicts interest.

Journal Pre-proof

Journal Pre-proof

Author contributions: L.F.P., T.S.J. and A.E. conceived the study. L.F.P. and P. Gasser performed most experiments. D.B. and P. Guntern performed animal work. All authors evaluated results and edited the manuscript. L.F.P., T.S.J and A.E. wrote the manuscript with input from all authors.

Funding: This research was supported by a grant from the Fondation Acteria (to A.E.), the Research Fund of the Swiss Lung Association, Bern and the Uniscientia foundation (to A.E.), and NIH grants AI115469 (to T.S.J.) and HL141493 (to T.S.J. and A.E.).

Acknowledgements: We thank all members of the Eggel and Jardetzky laboratories involved in this study. We further acknowledge Prof. Jean-Pierre Kinet for providing the transgenic mice expressing the human FcεRIα, Bühlmann Laboratories AG for scientific support, Prof. Peter M. Villiger, Prof. Britta Maurer, Dr. Monique Vogel and Prof. Martin Bachmann for granting access to equipment.

Journal Pre-proof

Journal Pre-proof

Abstract:

Background: Anaphylaxis represents one of the most severe and fatal forms of allergic reactions. Like most other allergies, it is caused upon activation of basophils and mast cells by allergen-mediated cross-linking of immunoglobulin E (IgE) bound to its high affinity receptor FcεRI on the cell surface. The systemic release of soluble mediators induces an inflammatory cascade rapidly causing symptoms with peak severity in minutes to hours after allergen exposure. Primary treatment for anaphylaxis consists of immediate intramuscular administration of adrenaline.

Objective: While adrenaline alleviates life-threatening symptoms of an anaphylactic reaction, there are currently no disease-modifying interventions available. Here, we sought to develop potent and fast acting IgE inhibitors with the potential to rapidly terminate acute allergic reactions.

Methods: Using affinity maturation by yeast display and structure-guided molecular engineering, we generated three optimized disruptive IgE inhibitors based on designed ankyrin repeat proteins (DARPins) and assessed their ability to actively remove IgE from allergic effector cells *in vitro* as well as in *in vivo* in mice.

Results: We report that the engineered IgE inhibitors rapidly dissociate preformed IgE:FcεRI complexes, terminate IgE-mediated signaling in pre-activated human blood basophils *in vitro* and shut down pre-initiated allergic reactions and anaphylaxis in mice *in vivo*.

Conclusions: Fast acting disruptive IgE inhibitors demonstrate the feasibility of developing kinetically optimized inhibitors for the treatment of anaphylaxis and the rapid desensitization of allergic individuals.

Journal Pre-proof

Key messages:

- Fast acting disruptive IgE inhibitors rapidly and systemically desensitize allergic effector cells.
- Pre-initiated anaphylaxis is significantly alleviated through application of fast acting disruptive IgE inhibitors.

Capsule Summary:

We engineered ultrapotent disruptive IgE inhibitors that desensitize allergic effector cells within minutes. Systemic application of the inhibitors resolves IgE-mediated anaphylaxis even post allergen exposure in vivo.

Key words: Active desensitization, affinity maturation, allergies, anaphylaxis, DARPins, disruptive IgE inhibitors, Fc-fusion, IgE, knobs-in-holes, yeast display.

Abbreviations: BMMC: bone marrow derived mast cells; $BMMC^{tg}$: bone marrow derived mast cells from transgenic mice expressing the human high affinity IgE receptor; DARPins: designed ankyrin repeat proteins; FcγRIIb: inhibitory IgG Fc-receptor; huFcεRIα: human high-affinity IgE receptor alpha chain subunit; huIgE: human immunoglobulin E; IgE: immunoglobulin E, JW8-IgE: 4-Hydroxy-3-iodo-5-nitrophenylacetyl hapten specific IgE; KIH: knobs-in-holes heterodimeric IgG1-Fc; NIP-BSA: 4-Hydroxy-3-iodo-5-nitrophenylacetyl hapten conjugated to bovine serum albumin.

Journal Pre-proof

Introduction:

While the number of annual hospitalizations due to anaphylactic reactions is difficult to track and varies considerably across geographic locations, a life-time prevalence of 0.05-2 % in the US and Europe has been estimated[1,2], and the frequency is on the rise[3]. Every year hundreds of patients die due to an unexpected episode of severe systemic anaphylaxis[4]. Mechanistically, an overwhelming amount of clinical and experimental evidence indicates that the predominant form of human anaphylaxis is immunoglobulin E (IgE) dependent[5]. The most common allergens inducing anaphylactic reactions are found in foods (e.g. peanuts, tree nuts, fish or shellfish), drugs (e.g antibiotics, nonsteroidal anti-inflammatory drugs, chemotherapeutic agents) or animal venoms (e.g. insect stings, snake bites)[6]. Antigen-mediated cross-linking of allergen-specific IgE bound to the high-affinity IgE receptor (FcεRI) on mast cells and basophils induces cellular degranulation and the immediate release of various preformed (e.g. histamine, tryptase, carboxypeptidase A, and proteoglycans), or de novo synthesized (e.g. prostaglandins, leukotrienes, platelet-activating factor and cytokines) soluble mediators[7,8]. Clinical symptoms secondary to degranulation peak in severity within minutes to an hour depending on the route of antigen exposure[2].

The universal first-line therapy for anaphylaxis is the immediate intramuscular application of adrenaline (i.e. epinephrine)[9]. Second- and third-line treatments consist of beta-2 agonist, anti-histamines or glucocorticoids[2]. These interventions rapidly alleviate the potentially fatal symptoms of anaphylaxis, but they do not interfere with the underlying pathomechanism of the disease. Currently, there is no suitable disease-modifying treatment option that acts fast enough to rapidly resolve the IgE-mediated allergic cascade. The therapeutic monoclonal anti-IgE antibody omalizumab (i.e. Xolair®), which is approved for the treatment of allergic asthma[10] and chronic spontaneous urticaria[11], has been shown to bind and neutralize free serum IgE[12]. However, with an average peak response of 12-16 weeks in allergic asthma[13] and 1-4 weeks in chronic spontaneous urticaria[14], the onset of action is too slow for use in acute anaphylaxis.

We previously described a novel class of kinetically disruptive IgE inhibitors[15] based on designed ankyrin repeat protein (DARPin) scaffolds[16,17]. These anti-IgE binders not only neutralize free IgE but actively remove pre-bound IgE from FcεRI on the surface of allergic effector cells. The fusion of a disruptive DARPin (E2_79) to a non-inhibitory anchor DARPin (E3_53) results in a bi-paratopic anti-IgE binder (bi53_79) with markedly enhanced disruptive

efficacy[18]. These observations led us to ask whether kinetically disruptive anti-IgE inhibitors could be developed with sufficient potency and activity to terminate an anaphylactic reaction. Using a directed evolution and a structure-guided approach, we have engineered highly potent disruptive IgE inhibitors based on DARPin scaffolds that rapidly desensitize pre-activated human allergic effector cells *in vitro* and resolve ongoing systemic IgE-dependent anaphylaxis *in vivo* in mice.

Methods

See the Methods section in this article's Online Repository at www.jacionline.org for detailed information about reagents, protein expression, crystallization, crystallographic data collection and refinement, yeast library construction, MACS and FACS selections, protein interaction measurements, cell culture models, western blotting, and mouse models for epicutaneous sensitization and passive systemic anaphylaxis.

Human samples and animals

Human blood donors were recruited at the Bern University Hospital with approval from the local ethics committee (KEK 2018-00204). Informed consent was obtained in accordance with the Helsinki Declaration. Mice that are transgenic for the human FcεRIα but lack the mouse FcεRIα (hu FcεRIα^{tg}) were obtained from Prof. Jean-Pierre Kinet. Double transgenic mice expressing human IgE and human FcεRIα (huIgE/huFcεRIα^{dtg}) were licensed from GenOway S.A. All animal experimentation was approved by the local animal committee (BE66/18).

Statistics

Statistical analysis and calculations described in the figure legends were carried out in Prism 8.0 software (GraphPad Software, La Jolla, Calif). In case of biological replicates, individual datapoints are shown. For technical duplicates and all other graphs, data are displayed as mean ± SEM.

Results:

Structural basis of IgE-anchoring by the non-competitive DARPin E3_53

To gain insight into the binding epitopes of the previously published bi-paratopic anti-IgE DARPin bi53_79[18], we crystallized IgE-Fc_{3-4} complexes with E3_53 and E2_79 (**Fig. 1, A and B; Fig. E1, A-D**) and solved the structure to a resolution of 2.8Å (**Table E1**). E3_53 binds IgE distal to the FcεRIα binding site and parallel to E2_79, placing it proximal to the CD23 binding site (**Fig. 1, A** and **Fig. E1, E-F**). Both DARPins bind IgE in similar N-C orientations (**Fig. 1, B)**. When fused to the E2_79 C-terminus E3_53 interferes with disruption activity, while E3_53 fused to the E2_79 N-terminus markedly enhances disruption[18]. This structure reveals that the nonfunctional C-terminal fusion (bi79_53) spans a longer solvent accessible surface distance (SASD) on a single IgE chain than N-terminal fusions, potentially accounting for its reduced activity relative to bi53_79 (**Table E2**).

The E3_53:IgE interface buries ~1000 $Å^2$ of surface area on each IgE chain across the Cε3 and Cε4 domains. The IgE Cε4 domain F-G loop protrudes prominently into a pocket formed by the N-terminal capping domain, internal-repeat 1 (IR1), and internal-repeat 2 (IR2) of E3_53 (**Fig. 1, C**). This positions IgE-P533 in a hydrophobic pocket adjacent to E3_53-T48, L53, Y56, and L86 (**Fig. 1, D**). Internal-repeat 3 (IR3) makes extensive contacts with IgE, including a salt bridge between IgE-R525 and E3_53-D111, and multiple hydrogen bonds with both the AB and EF helices of Cε3 (**Fig. 1, C**). Interactions also occur within the invariant E3_53 C-terminal capping domain, including a salt bridge between IgE-K352 and D156 of E3_53, and interactions between E3_53-F145 and a hydrophobic patch formed in Cε3 by F346, I350, and R351 (**Fig. 1, C**). E2_79 interactions with IgE are similar to those observed in a previously determined structure[15].

IgE exhibits conformational flexibility in its Cε3 domains relative to the stable Cε4 dimer. The flexible Cε3 domains adopt an open conformation when binding to the FcεRIα[19,20], while CD23-bound IgE adopts a closed conformation[21]. These receptor interactions are mutually exclusive [22,23]. Although E3_53 does not compete with FcεRIα, the structure reveals that it interacts with both Cε3 and Cε4 domains, raising the possibility that E3_53 could act as a partial allosteric modulator and enhance bi53_79 disruptive activity. Comparison of E3_53:IgE interface residues in the FcεRIα complex (open) and the E3_53 complex (closed) shows minor displacements in the E3_53 epitope within the Cε3 AB and EF helices (**Fig. 1, D**). In contrast, a major portion of CD23 interactions, a known allosteric modulator, occurs with the mobile Cε3 CD loop (**Fig. 1, E-F**).

Journal Pre-proof

To examine the impact of IgE conformational changes on E3_53 interactions, we measured the kinetics of E3_53 binding to free IgE and IgE:FcεRIα complexes (**Fig. 1, G** and **Table E3**). E3_53 dissociates slightly faster from IgE:FcεRIα complexes, yet has a similar affinity for both free and receptor bound IgE, consistent with prior assays[24]. We also determined the half-maximal disruptive concentrations (DC_{50}) of E3_53, E2_79, a mix of E2_79 and E3_53, and bi53_79. FcεRIα coupled beads were loaded with biotinylated-IgE-Fc_{2-4} (bIgE-Fc_{2-4}), washed, and treated with each agent or mix of agents and assayed for remaining bIgE-Fc_{2-4} (**Fig. 1, H**). The E2_79 DC_{50} is modestly improved in the presence of soluble E3_53 but is dramatically improved when covalently fused to E3_53 in bi53_79. E3_53 slightly enhances the loss of bead-bound IgE alone. These results confirm that E3_53 primarily acts by anchoring E2_79 to complexes in bivalent molecules, but it may also be a weak allosteric modulator or catalyst for E2_79 mediated disruption.

High affinity anchoring domains increase disruptive potency

Given the anchoring role of E3_53 in enhancing bi53_79 disruptive activity, we hypothesized that increasing the dwell time of E3_53 on IgE:FcεRIα complexes could further improve the potency of bi53_79. We therefore engineered a high affinity E3_53 variant using yeast display (**Fig. 2, A**). A ~3.0 x 10^8 transformant error prone library was generated from E3_53, using a T48N mutation to remove a potential N-linked glycosylation site. Libraries were incubated with preformed bIgE-Fc_{2-4}:FcεRIα complexes, washed, and then exposed to unlabeled IgE for 1-4 hours to isolate slowly dissociating variants retaining bIgE-Fc_{2-4} over five rounds of selection (**Fig. 2, A**). These selections dramatically slowed the effective off-rate of bIgE-Fc_{2-4}:FcεRIα complexes in competitive binding experiments on yeast (**Fig. E2, A**). After five rounds, a shuffled mutant library was generated to enrich for favorable and exclude unfavorable mutations (**Fig. E2, B and C**). Following a further selection round, clone E07 was chosen for characterization based on the number of enriched mutations (**Fig. 2, C**). Mutations at the interface were modeled into the E3_53 structure revealing new polar interactions, as well as mutations that likely induce more complex rearrangements of neighboring residues (**Fig. E2, D and E).** E07 showed enhanced binding affinity to free IgE and IgE:FcεRIα complexes, primarily driven by a 7-10-fold slower dissociation rate (**Fig. 2, C and Table E3**). E07 maintains a similar preference for free IgE as E3_53, with ~2-fold weaker binding to intact IgE:FcεRIα complexes.

We produced E07 N-terminal fusions to E2_79 (**Fig. E3, A and B**) and the resulting biE07_79 showed significantly improved IgE disruption in bead-based and SPR assays (**Fig. 2, D and E**). Although the half-maximal disruptive concentration (DC_{50}) of biE07_79 was lowered, IgE release plateaued prior to achieving full dissociation obtained with E2_79 or bi53_79 in bead-based assays (**Fig. 2, D**). In SPR experiments, a similar effect is observed despite the shorter contact times and continuous flow (**Fig. 2, E**), although the SPR signals are confounded by concurrent formation of inhibitor:IgE:FcεRIα complexes. However, the enhanced DC_{50} directly correlates with the increased affinity of the E07 anchoring domain (**Fig. E3, C**).

We next assessed whether biE07_79 is superior to bi53_79 in desensitizing allergic effector cells. We generated bone marrow derived mast cells from human FcεRIα transgenic mice ($BMMC^{tg}$, **Fig. E3, D**) and loaded them with human NIP-specific JW8-IgE, treated them for 30 minutes with increasing concentrations of bi53_79 or biE07_79 and subsequently stimulated with NIP-BSA. While biE07_79 reduced cell surface IgE levels and inhibited antigen-mediated cell activation more efficiently than bi53_79 (**Fig. 2, F and H and Fig. E3, E and F**), it also induced spontaneous activation of the $BMMC^{tg}$ without NIP-BSA stimulation (**Fig. 2, G and Fig. E3, G**). These results suggest that biE07_79 induces cell activation in the absence of antigen by crosslinking IgE:FcεRIα complexes. Since we did not observe spontaneous activation with bi53_79 this anaphylactogenicity is directly related to the affinity of the E07 anchoring domain.

Linker redesign and FcγRIIb targeting improves IgE disruptive activity and effector cell inhibition, while eliminating intrinsic anaphylactogenicity

Anaphylactogenicity of biE07_79 could be caused by the more stable dwell time of the E07 anchor enabling the binding and crosslinking of neighboring IgE:FcεRI complexes through the E2_79 domain. We therefore reengineered the original 20 AA long (G4S)4 linker to reduce the possibility of receptor crosslinking by truncating the linker to (G4S)2, yet the truncation reduced disruptive activity and induced higher anaphylactogenicity compared to the original biE07_79 (**Fig. E4, A-C**). We next sought to geometrically constrain the relative positions of the anchoring and disruptive modules through a knobs-in-holes (KIH), heterodimeric IgG_1-Fc fusion strategy. For this second approach, short linkers were used to fuse E07 and E2_79 DARPins to the C-termini of the KIH IgG_1-Fc, which aligned well with the N-termini of the two DARPins (**Fig. 3, A**). The KIH_E07_79 construct not only provides a more structured linker between the two

DARPins, but it also introduces the possibility for the IgG_1-Fc to engage inhibitory FcγRIIb receptors present on allergic effector cells and thereby further suppress potential anaphylactogenicity[24]. To examine the impact of binding FcyRIIb independently from the structured positioning of E2_79 and E07 in the KIH construct, we generated two additional trivalent DARPins. We fused the FcγRIIb-specific DARPin D11[25] to the N-terminus of bi53_79 and biE07_79 to generate trivalent variants (tri11_53_79 and tri11_E07_79) with the (G4S)4 linker (**Fig. 3, A**). KIH_E07_79 showed increased disruptive activity and lower plateau in bead- and SPR-based assays while both trivalent variants showed reduced disruptive efficacy (**Fig. 3, B and C**) compared to their bivalent counterparts (**Fig. 2, D and E**).

All three proteins (KIH_E07_79, tri11_53_79 and tri11_E07_79) were non-anaphylactogenic in $BMMC^{tg}$ (**Fig. 3, D and E5, A and B**), even though D11 has a 1000-fold lower affinity for murine FcγRIIb compared to its ~1.9nM K_D for the human receptor. Consistent with results from bead-based and SPR IgE stripping assays, KIH_E07_79 removed IgE with higher efficacy than tri11_53_79 or tri11_E07_79 in cell-based ($BMMC^{tg}$) assays (**Fig. 3, D and Fig. E5, C**). It stripped IgE from cells within 30 minutes and showed the highest inhibitory potency in blocking antigen-induced $BMMC^{tg}$ activation at concentrations as low as 4-20 nM (**Fig. 3, D and Fig. E5, D**). Together, these data indicate that conformational positioning of the anchoring and disruptive domains on the IgG_1-Fc scaffold enhances intrinsic IgE disruption activity and eliminates anaphylactogenicity of bispecific anti-IgE binders. In addition, the loss in disruptive efficacy of the trivalent DARPins is significantly compensated for by FcγRIIb engagement.

We next compared the activities of these constructs using primary human basophils isolated from grass-allergic patients (**Fig. E6**, **A**). To examine the impact of human FcγRIIb, basophils were incubated with tri11_53_79, tri11_07_79 or KIH_E07_79 with and without prior blocking of FcγRIIb. As observed on $BMMC^{tg}$ (**Fig. 2, H**), biE07_79 was also anaphylactogenic on isolated primary human basophils (**Fig. E7**). In contrast, KIH_E07_79, tri11_53_79 and tri11_07_79 did not activate human basophils, even in the presence of FcγRIIb blocking (**Fig. 3, E and Fig. E6, B**). The trivalent DARPins and KIH_E07_79 were remarkably more efficient in stripping IgE than biE07_79 or omalizumab (**Fig. 3, E**, **Fig. E7 and Fig. E6, C**) and blocking of FcγRIIb partially reduced their potency (**Fig. 3, E**). These results indicate that co-engagement of human FcγRIIb with both high affinity (i.e. DARPin D11) and low affinity (i.e. IgG1-Fc) domains increases the disruptive efficacy of the inhibitors. Notably, the relatively weaker IgE stripping by

the trivalent DARPins in the murine BMMC^{tg} is greatly improved in the presence of the high affinity D11 interaction with human FcγRIIb in the basophils.

To assess the impact of the different variants on human primary basophil activation, we stimulated isolated basophils with a 6-grass allergen mix after 30 minutes of inhibitor treatment (**Fig. 3, E and Fig. E6, D**). Neither biE07_79 nor omalizumab showed any inhibition of basophil activation in this experimental setup (**Fig. E7**). However, KIH_E07_79, tri11_53_79 and tri11_E07_79 all abrogated allergen-mediated basophil activation at low nanomolar concentrations (**Fig. 3, E, and Fig. E6, D**). Blocking of FcγRIIb partially reversed the inhibition, which could depend on enhanced FcγRIIb-mediated recruitment to the basophils surface or on inhibitory signaling through FcγRIIb ITIMs. To examine potential induction of negative signaling events, we assessed intracellular FcγRIIb phosphorylation in the presence of the inhibitors with or without FcγRIIb blocking (**Fig. 3, F**). Both trivalent constructs but not KIH_E07_79 induced an inhibitory signal through FcγRIIb phosphorylation[25,26]. In summary, all three constructs are highly efficient in removing IgE from human primary basophils. Furthermore, the data indicate that the trivalent inhibitors exhibit increased potency on human cells through activation of inhibitory FcγRIIb signaling.

KIH_E07_79 rapidly desensitizes allergic effector cells and resolves ongoing anaphylaxis in mice.

We selected KIH_E07_79 to assess *in vivo* efficacy in mice, because it showed the most potent activity in BMMC^{tg} assays. In addition, the KIH_E07_79 IgG_1-Fc domains might interact with the murine neonatal Fc-receptor, extending serum half-life in mice[27,28]. Omalizumab was used as a benchmark in these studies. Double transgenic mice expressing human IgE and human FcεRIα were epicutaneously sensitized with ovalbumin by daily topical co-application with the vitamin D analogue MC903 (**Fig. 4, A**). This model has been shown to induce a strong T_h2 response leading to systemic sensitization with expanded eosinophil, basophil and mast cell pools[29-31]. Sensitized mice received one injection of either KIH_E07_79, omalizumab or PBS on day 14. Compared to EtOH control treated mice, sensitization with MC903 and OVA significantly increased free blood plasma IgE and cell surface IgE levels on blood basophils (**Fig. 4, B and C**) and the sensitization of animals across groups was similar prior to anti-IgE treatment on day 12 (**Fig. 4, D-F**). In contrast, free plasma IgE levels were suppressed 9 hours after injection (i.e. day

15) with both KIH_E07_79 and omalizumab (**Fig. 4, G and H**), but only KIH_E07_79 rapidly reduced cell surface IgE on blood basophils to baseline levels in this short time period (**Fig. 4, I and Fig. E8, A**). We also quantified IgE levels on mast cells close to the injection site in the peritoneum (PEC) or on basophils and mast cells distant from the injection site in lung, ear skin or back skin. While omalizumab showed no decrease in surface IgE compared to the PBS control group upon treatment, KIH_E07_79 significantly reduced IgE levels on basophils and mast cells from all tissue sources (**Fig. 4, J-M and Fig. E8, B-E**). These data indicate that KIH_E07_79 is a fast acting disruptive IgE inhibitor that rapidly desensitizes allergic effector cells in circulation and peripheral tissues *in vivo*.

Given the remarkable efficacy of systemic desensitization with KIH_E07_79, we sought to test its immediate impact on acute anaphylactic reactions. First, we assessed whether it has the ability to interfere with IgE-dependent cell degranulation post allergen stimulation in vitro. For this purpose, we sensitized $BMMC^{tg}$ with recombinant human NIP-specific JW8-IgE, challenged the cells with NIP-BSA and added either KIH_E07_79 or omalizumab at different concentrations 5 minutes later. Cell activation was quantified 25 minutes after allergen stimulation by measuring CD107a expression (**Fig. 5, A and Fig. E9, A**). While KIH_E07_79 dose-dependently inhibited $BMMC^{tg}$ activation in this setup, omalizumab showed no effect. Next, we tested how KIH_E07_79 performs when given after antigen challenge in a passive systemic anaphylaxis model in human FcεRIα transgenic mice (**Fig. 5, B**). The mice received one injection of recombinant human NIP-specific JW8-IgE to systemically sensitize allergic effector cells. The next day, they were challenged with NIP-BSA antigen to induce systemic anaphylaxis. KIH_E07_79, omalizumab or PBS were injected 5 minutes post antigen stimulation. As a read-out for systemic anaphylaxis, we measured changes in body core temperature over 2 hours (**Fig. 5, B**). KIH_E07_79 treatment significantly reduced the maximal drop in body core temperature and shortened the recovery time, while there was no significant difference observed between the PBS and omalizumab treated groups. The area under the curve for the body core temperature measurements confirm a significantly lower anaphylactic reaction in mice receiving KIH_E07_79 (**Fig. 5, B**).

Finally, to investigate whether KIH_E07_79 may also resolve an ongoing allergic reaction in human cells, we isolated primary human basophils from allergic donors and stimulated them with grass-mix allergen. The cells were treated either 5 or 25 minutes post allergen challenge

with KIH_E07_79, omalizumab or PBS and activation was measured by CD63 surface expression and leukotriene LTC4 release 50 minutes after allergen stimulation (**Fig. 5, C**). Both CD63 surface expression and LTC4 release were inhibited by KIH_E07_79 treatment 5 minutes post allergen challenge (**Fig. 5, D and Fig. E9, B**), while omalizumab treatment had no effect. At 25 minutes post allergen challenge KIH_E07_79 treatment no longer suppressed activation (**Fig. 5, E**). To determine whether inhibition can also be observed in the presence of physiological levels of free IgE, we collected whole blood of three grass allergic patients with up to 533 kU/l total IgE and performed a KIH_E07_79 dose titration 5 minutes post allergen challenge (**Fig. 5, F**). KIH_E07_79 suppressed basophil activation after allergen stimulation at concentrations higher than 100 nM (**Fig. 5, G and Fig. E9, C**). Importantly, without allergen challenge KIH_E07_79 treatment alone does not activate basophils (**Fig. 5, H**). To determine the window of opportunity for KIH_E07_79 to suppress basophil activation, KIH_E07_79 was added to the whole blood at different time points after allergen activation (**Fig. 5, I**). Significant suppression of basophil activation was achieved up to 10 minutes post allergen stimulation (**Fig. 5, J**).

Basophils release pre-stored granular mediators (e.g. histamine) and *de novo* produced arachidonic acid derived products (e.g. leukotrienes and prostaglandins) within minutes after IgE-dependent stimulation[32]. However, *de novo* synthesized cytokines are released with slower kinetics with IL-4 peaking at 4-6 hours and IL-13 at 24 hours post IgE cross-linking[33,34]. These mediators are important for the allergic late phase reaction as they are involved in the recruitment and activation of inflammatory cells[35]. Using isolated basophils, we tested whether KIH_E07_79 could inhibit release of *de novo* synthesized IL-13, when applied post allergen challenge. Indeed, IL-13 release was significantly suppressed at 5 and even at 25 minutes after allergen challenge (**Fig. 5, K and L**). KIH_E07_79 can evidently interfere with FcεRI signaling that drives both early and late phase reactions and suppress de novo cytokine biosynthesis over a longer time window after antigen activation. Together, these results demonstrate the remarkable potency of KIH_E07_79 to rapidly terminate pre-initiated allergic effector cell signaling consistent with its ability to systemically block acute allergic anaphylaxis.

Discussion

We have applied structural, biophysical and immunological studies to engineer bivalent anti-IgE agents that can rapidly disarm effector cells to interrupt a pre-initiated allergic signaling cascade.

These bivalent inhibitors act by localizing an inhibitory anti-IgE DARPin (E2_79) proximal to the IgE:FcεRI interface using a second non-inhibitory anti-IgE DARPin (E3_53 or E07) as an anchor to the receptor complex. This anchoring approach enhances the ability of E2_79 to bind to IgE within the complex and accelerate IgE dissociation from FcεRI. We reasoned that increasing the affinity of the anchoring domain could improve the disruptive potency of bivalent IgE inhibitors, which is borne out by our experiments with the affinity matured E07 variant of E3_53. However, increasing anchor affinity also resulted in inhibitors that spontaneously activated effector cells. Further rounds of inhibitor engineering revealed that positioning the two DARPin domains using an IgG-Fc scaffold and engagement of FcγRIIb inhibitory receptors both eliminated the spontaneous activation of effector cells and increased the potency of IgE:FcεRI complex disruption. Our resulting inhibitor, KIH_E07_79, strips IgE from cell surface receptors in minutes at low nanomolar concentrations and interrupts both early and late phases of allergic cell activation after allergen-initiated signaling has commenced.

Targeting IgE:FcεRI complexes on mast cells or basophils with inhibitors raises the possibility of inadvertently triggering these cells through receptor crosslinking. Here we observed that increasing the affinity of our anchoring DARPin from bi53_79 to biE07_79 resulted in spontaneous activation. This is likely due to receptor crosslinking and/or the formation of stable non-disrupted inhibitor-IgE complexes, which is enabled by a flexible glycine/serine interdomain linker. In one approach to suppress this activation, we fused D11, a high affinity FcγRIIb targeting DARPin, to the bivalent DARPins to yield tri11_53_79 and tri11_E07_79. Both trivalent inhibitors exhibit worse disruptive potency than their bivalent counterparts in biochemical assays and failed to fully dissociate IgE:FcεRI complexes. However, the trivalent molecules induce inhibitory signaling in human cells and localize to the cell surface via high affinity binding of D11 to FcγRIIb, which dramatically increased their potency in cells. We previously showed that co-ligation of FcγRIIb with FcεRI is required for inhibitory activity[25]. Both tri11_53_79 and tri11_E07_79 induce phosphorylation of FcγRIIb ITIMs on human cells, consistent with the interpretation that their slower disruption kinetics allows FcεRI:FcγRIIb crosslinking.

We also used our structure of the IgE:E2_79:E3_53 complex to design a C-terminal knob-in-hole IgG_1-Fc fusion (KIH_E07_79) to suppress anaphylactogenicity by restricting the positioning of the two DARPin domains. With KIH_E07_79, we observe near complete dissociation of IgE

receptor complexes in biochemical assays. The potency of KIH_E07_79 is further enhanced by interactions with FcγRIIb on basophils, as a blockade of FcγRIIb reduces IgE stripping and potency. However, in contrast to the trivalent DARPins, KIH_E07_79 does not induce active inhibitory signaling through FcγRIIb phosphorylation. The reason for this difference is likely twofold. First the IgG_1-Fc binds to FcγRIIb with low micromolar affinity, over 1000-times weaker than the DARPin D11[25,36]. Second, KIH_E07_79 exhibits more rapid and complete disruption of IgE:FcεRI complexes in biochemical assays, reducing the possibility of co-ligating FcγRIIb and IgE:FcεRI complexes.

KIH_E07_79 demonstrates the potential for an anti-IgE agent to act as a rescue therapy for acute allergic reactions and terminate pathologic IgE-mediated inflammatory responses. KIH_E07_79 inhibits degranulation of human basophils within a ten-minute window post allergen exposure. After ten minutes, KIH_E07_79 treatment no longer prevents degranulation. However, the release of *de novo* synthesized IL-13 remained significantly inhibited by KIH_E07_79 up to 25 minutes after basophil activation, indicating that persistent IgE signaling may be required for *de novo* mediator synthesis. Consistent with these observations real time measurements of calcium flux in human mast cells suggests that IgE signaling induces sustained intracellular calcium flux for at least 30 minutes[37] and the phosphorylation of NFAT and transcription of multiple cytokines occur on similar timeframes[38,39]. While the release of pre-stored and rapidly synthesized mediators during anaphylaxis may always require ultrafast interventions, our data suggest that IgE disruption can aid in suppressing the synthesis of *de novo* allergic mediators like IL-13 after allergen exposure even at later time points. Blockade of these events may have important therapeutic implications given the role of basophil and mast cell derived cytokines in perpetuating allergic immune polarization and IgE production upon repeated allergen exposure[40,41].

Although DARPins are small artificial binding proteins with a limited clinical history as compared to monoclonal antibodies, multiple DARPins have now entered human trials[42-44]. KIH_E07_79 is a IgG_1-Fc fusion and should exhibit enhanced serum half-life and tissue transport *in vivo* as compared to individual DARPins[45]. While an IgE inhibitor is unlikely to completely supplant auto-injectable adrenaline in the management of anaphylaxis, the rapid and complete inhibition of IgE mediated signaling could be used as an adjunct therapy or to accelerate the management of a wide range of allergic disorders.

415

Journal Pre-proof

References:

1. Yu JE, Lin RY. The Epidemiology of Anaphylaxis. Clinical reviews in allergy & immunology 2015;54:366–74.

2. Muraro A, Roberts G, Worm M, Bilò MB, Brockow K, Fernandez-Rivas M, et al. Anaphylaxis: guidelines from the European Academy of Allergy and Clinical Immunology. Allergy2014;69:1026–45.

3. Simons FER, Ebisawa M, Sánchez-Borges M, Thong BY, Worm M, Tanno LK, et al. 2015 update of the evidence base: World Allergy Organization anaphylaxis guidelines. World Allergy Organ J 2015;8:1–16.

4. Turner PJ, Jerschow E, Umasunthar T, Lin R, Campbell DE, Boyle RJ. Fatal Anaphylaxis: Mortality Rate and Risk Factors. J Allergy Clin Immunol Pract 2017;5:1169–78.

5. Finkelman FD. Anaphylaxis: lessons from mouse models. Journal of allergy and clinical immunology 2007;120:506–15–quiz516–7.

6. Kemp SF, Lockey RF. Anaphylaxis: A review of causes and mechanisms. Journal of allergy and clinical immunology 2002;110:341–8.

7. Metcalfe DD, Peavy RD, Gilfillan AM. Mechanisms of mast cell signaling in anaphylaxis. J Allergy Clin Immunol 2009;124:639–46–quiz647–8.

8. Reber LL, Hernandez JD, Galli SJ. The pathophysiology of anaphylaxis. J Allergy Clin Immunol 2017;140:335–48.

9. Sampson HA, Muñoz-Furlong A, Bock SA, Schmitt C, Bass R, Chowdhury BA, et al. Symposium on the definition and management of anaphylaxis: summary report. 2005. pages 584–91.

10. Busse W, Corren J, Lanier BQ, McAlary M, Fowler-Taylor A, Cioppa GD, et al. Omalizumab, anti-IgE recombinant humanized monoclonal antibody, for the treatment of severe allergic asthma. Journal of allergy and clinical immunology 2001;108:184–90.

11. PhD TWC, BS CC, PhD C-JL, MD MM, DSc MKCP, MD MM. The potential pharmacologic mechanisms of omalizumab in patients with chronic spontaneous urticaria. Journal of allergy and clinical immunology 2014;:1–8.

12. Gasser P, Eggel A. Targeting IgE in allergic disease. Curr Opin Immunol 2018;54:86–92.

13. Holgate S, Buhl R, Bousquet J, Smith N, Panahloo Z, Jimenez P. The use of omalizumab in the treatment of severe allergic asthma: A clinical experience update. Respir Med 2009;103:1098–113.

14. Metz M, Ohanyan T, Church MK, Maurer M. Omalizumab is an effective and rapidly acting therapy in difficult-to-treat chronic urticaria: A retrospective clinical analysis. Journal of Dermatological Science 2013;:1–6.

15. Kim B, Eggel A, Tarchevskaya SS, Vogel M, Prinz H, Jardetzky TS. Accelerated disassembly of IgE-receptor complexes by a disruptive macromolecular inhibitor. Nature 2012;:1–7.

16. Binz HK, Stumpp MT, Forrer P, Amstutz P, Plückthun A. Designing repeat proteins: well-expressed, soluble and stable proteins from combinatorial libraries of consensus ankyrin repeat proteins. J Mol Biol 2003;332:489–503.

17. Binz HK, Amstutz P, Kohl A, Stumpp MT, Briand C, Forrer P, et al. High-affinity binders selected from designed ankyrin repeat protein libraries. Nat Biotechnol 2004;22:575–82.

18. Eggel A, Baravalle G, Hobi G, Kim B, Buschor P, Forrer P, et al. Accelerated dissociation of IgE-FcεRI complexes by disruptive inhibitors actively desensitizes allergic effector cells. J Allergy Clin Immunol 2014;133:1709–19.e8.

19. Garman SC, Wurzburg BA, Tarchevskaya SS, Kinet JP, Jardetzky TS. Structure of the Fc fragment of human IgE bound to its high-affinity receptor Fc epsilonRI alpha. Nature 2000;406:259–66.

20. Wurzburg BA, Garman SC, Jardetzky TS. Structure of the human IgE-Fc C epsilon 3-C epsilon 4 reveals conformational flexibility in the antibody effector domains. Immunity 2000;13:375–85.

21. Wurzburg BA, Kim B, Tarchevskaya SS, Eggel A, Vogel M, Jardetzky TS. An engineered disulfide bond reversibly traps the IgE-Fc3-4 in a closed, non-receptor binding conformation. Journal of Biological Chemistry 2012;

22. Dhaliwal B, Yuan D, Pang MOY, Henry AJ, Cain K, Oxbrow A, et al. Crystal structure of IgE bound to its B-cell receptor CD23 reveals a mechanism of reciprocal allosteric inhibition with high affinity receptor Fc RI. Proc Natl Acad Sci USA 2012;109:12686–91.

23. Borthakur S, Hibbert RG, Pang MOY, Yahya N, Bax HJ, Kao MW, et al. Mapping of the CD23 binding site on IgE and allosteric control of the IgE-Fc RI interaction. Journal of Biological Chemistry 2012;

24. Eggel A, Buschor P, Baumann MJ, Amstutz P, Stadler BM, Vogel M. Inhibition of ongoing allergic reactions using a novel anti-IgE DARPin-Fc fusion protein. Allergy 2011;66:961–8.

25. Zellweger F, Gasser P, Brigger D, Buschor P, Vogel M, Eggel A. A novel bispecific DARPin targeting FcγRIIB and FcεRI-bound IgE inhibits allergic responses. Allergy 2016;72:1174–83.

26. Malbec O, Cassard L, Albanesi M, Jönsson F, Mancardi D, Chicanne G, et al. Trans-inhibition of activation and proliferation signals by Fc receptors in mast cells and basophils. Science Signaling 2016;9:ra126–6.

27. Suzuki T, Ishii-Watabe A, Tada M, Kobayashi T, Kanayasu-Toyoda T, Kawanishi T, et al. Importance of Neonatal FcR in Regulating the Serum Half-Life of Therapeutic Proteins Containing the Fc Domain of Human IgG1: A Comparative Study of the Affinity of Monoclonal Antibodies and Fc-Fusion Proteins to Human Neonatal FcR. J Immunol 2010;184:1968–76.

28. Unverdorben F, Richter F, Hutt M, Seifert O, Malinge P, Fischer N, et al. Pharmacokinetic properties of IgG and various Fc fusion proteins in mice. MAbs 2016;8:120–8.

29. Zhang Z, Hener P, Frossard N, Kato S, Metzger D, Li M, et al. Thymic stromal lymphopoietin overproduced by keratinocytes in mouse skin aggravates experimental asthma. Proceedings of the National Academy of Sciences 2009;106:1536–41.

30. Noti M, Kim BS, Siracusa MC, Rak GD, Kubo M, Moghaddam AE, et al. Exposure to food allergens through inflamed skin promotes intestinal food allergy through the thymic stromal lymphopoietin-basophil axis. J Allergy Clin Immunol 2014;133:1390–6.

31. Noti M, Wojno EDT, Kim BS, Siracusa MC, Giacomin PR, Nair MG, et al. Thymic stromal lymphopoietin–elicited basophil responses promote eosinophilic esophagitis. Nat Med 2013;19:1–11.

32. Miura K, Schroeder JT, Hubbard WC, MacGlashan DW. Extracellular signal-regulated kinases regulate leukotriene C4 generation, but not histamine release or IL-4 production from human basophils. J Immunol 1999;162:4198–206.

33. Redrup AC, Howard BP, MacGlashan DW, Kagey-Sobotka A, Lichtenstein LM, Schroeder JT. Differential regulation of IL-4 and IL-13 secretion by human basophils: their relationship to histamine release in mixed leukocyte cultures. J Immunol 1998;160:1957–64.

34. Gibbs BF, HAAS H, Falcone FH, Albrecht C, Vollrath IB, Noll T, et al. Purified human peripheral blood basophils release interleukin-13 and preformed interleukin-4 following immunological activation. Eur J Immunol 1996;26:2493–8.

35. White M. Mediators of inflammation and the inflammatory process. Journal of allergy and clinical immunology 1999;103:S378–81.

36. Bruhns P. Properties of mouse and human IgG receptors and their contribution to disease models. Blood 2012;119:5640–9.

37. Gaudenzio N, Sibilano R, Marichal T, Starkl P, Reber LL, Cenac N, et al. Different activation signals induce distinct mast cell degranulation strategies. J Clin Invest 2016;126:3981–98.

38. Lorentz A, Schwengberg S, Sellge G, Manns MP, Bischoff SC. Human Intestinal Mast Cells Are Capable of Producing Different Cytokine Profiles: Role of IgE Receptor Cross-Linking and IL-4. J Immunol 2000;164:43–8.

39. Hutchinson LE, McCloskey MA. FcεRI-mediated Induction of Nuclear Factor of Activated T-cells *. J Biol Chem 1995;270:16333–8.

40. Ryzhov S, Goldstein AE, Matafonov A, Zeng D, Biaggioni I, Feoktistov I. Adenosine-Activated Mast Cells Induce IgE Synthesis by B Lymphocytes: An A2B-Mediated Process Involving Th2 Cytokines IL-4 and IL-13 with Implications for Asthma. J Immunol 2004;172:7726–33.

41. Asrat S, Kaur N, Liu X, Ben L-H, Kajimura D, Murphy AJ, et al. Chronic allergen exposure drives accumulation of long-lived IgE plasma cells in the bone marrow, giving rise to serological memory. Sci Immunol 2020;5:eaav8402.

42. Kunimoto D, Yoon YH, Wykoff CC, Chang A, Khurana RN, Maturi RK, et al. Efficacy and Safety of Abicipar in Neovascular Age-Related Macular Degeneration: 52-Week Results of Phase 3 Randomized Controlled Study. Ophthalmology 2020;127:1331–44.

43. Walser M, Rothenberger S, Hurdiss DL, Schlegel A, Calabro V, Fontaine S, et al. Highly potent anti-SARS-CoV-2 multi-DARPin therapeutic candidates. bioRxiv 2020;584:2020.08.25.256339.

44. Stumpp MT, Dawson KM, Binz HK. Beyond Antibodies: The DARPin ® Drug Platform. BioDrugs 2020;34:423–33.

45. Steiner D, Merz FW, Sonderegger I, Gulotti-Georgieva M, Villemagne D, Phillips DJ, et al. Half-life extension using serum albumin-binding DARPin® domains. Protein Eng Des Sel 2017;30:583–91.

Journal Pre-proof

Figure 1. Structure of E3_53 and E2_79 in complex with IgE-Fc3-4. (A) IgE-Fc_{3-4}:E3_53:E2_79 complex. **(B)** Relative positions of E2_79 and E3_53 DARPin N/C-term capping and internal repeat (IR) domains. **(C)** Detailed views of E3_53(green):IgE(grey) interface showing polar interactions or hydrogen bonds (black dashes). **(D)** A single chain of IgE-Fc_{3-4} from the IgE-Fc_{3-4}:E3_53:E2_79 complex (green) aligned to site-2-proximal Cε4 domain of the FcεRIα:IgE-Fc_{3-4} complex (grey). (Inset) displacement of IgE-Cα residues at the E3_53:IgE interface (black arrows). **(E)** Comparison of E3_53 and CD23 footprints on IgE-Fc_{3-4}. **(F)** Relative position of CD23 to a single chain of IgE-Fc_{3-4} from the CD23:IgE-Fc_{3-4} complex (yellow) aligned to the site-2-proximal Cε4 of the IgE-Fc_{3-4}:FcεRIα complex (grey). (Inset) displacement of IgE-Cα residues at the CD23:IgE interface (black arrows). **(G)** Binding kinetics of E3_53 to free IgE or IgE immobilized on FcεRIα as assessed by BLI. **(H)** Disruption of bIgE-Fc_{2-4} immobilized on FcεRIα functionalized beads after a 30-minute incubation with indicated anti-IgE agent. Data is shown as mean ± SEM.

Figure 2. Affinity maturation of E3_53. (A) Schematic of the yeast-based selection scheme. **(B)** Mutations observed in E07, and their position in (Y) or outside of (N) the E3_53:IgE interface. The N48D* mutation in E07 arose from the parental library T48N mutant. **(C)** Binding kinetics of E07 to free IgE or IgE immobilized on FcεRIα as assessed by BLI. **(D)** Disruption of bIgE-Fc_{2-4} immobilized on FcεRIα functionalized beads after 30 minutes with indicated anti-IgE. **(E)** SPR disruption assay, with Sus11-IgE immobilized on FcεRIα exposed to anti-IgE agents. (**F-G)** $BMMC^{tg}$ loaded with 3 nM JW8-IgE and treated for 30 minutes with IgE inhibitors at the indicated concentrations and assessed for (**F**) IgE stripping (desensitization) and (**G**) spontaneous activation (anaphylactogenicity). After treatment cells were stimulated with 100 ng/ml NIP(7)-BSA for 30 minutes and then assessed for (**G**) activation (antigen activation). Assays (**F-H**) were performed with the same cells and in technical duplicates. Data is shown as mean ± SEM.

Figure 3. Engineering novel linkers and fusions for bivalent disruptive inhibitors. (A) Schematic of novel linkers and fusions. **(B)** Disruption of bIgE-Fc_{2-4} immobilized on FcεRIα beads after 30 minutes with anti-IgE agents. **(C)** SPR disruption assay, with Sus11-IgE immobilized on FcεRIα exposed to anti-IgE agents. **(D)** $BMMC^{tg}$ loaded with JW8-IgE and

treated for 30 minutes with anti-IgE agents, assessed for activation ($CD107a^+$) (anaphylactogenicity) or IgE stripping (desensitization). After treatment cells were stimulated with NIP(7)-BSA for 30 minutes and then assessed for activation ($CD107a^+$) (antigen activation). All assays in (**D**) were performed with the same cells and in technical duplicates. **(E)** Basophils from allergic donors (n = 4) were treated for 30 minutes with anti-IgE agents, assessed for activation ($CD63^+$) (anaphylactogenicity) or IgE stripping (desensitization). After treatment cells were stimulated with a predetermined EC_{opt} of 6-grass allergen mix for 30 minutes and assessed for activation ($CD63^+$) (antigen activation). Assays were conducted with or without DARPin D11 FcγRIIb blockade. **(F)** Allergen stimulated cells from **(E)** were lysed and analyzed for phosphorylation of FcγRIIb (pFcγRIIb). GAPDH is shown as loading control. Data in **(B and D)** is shown as mean ± SEM. In **(E)** individual datapoints and mean ± SEM are shown.

Figure 4. KIH_E07_79 rapidly desensitizes basophils and mast cells *in vivo*. (A) huIgE/huFcεRIα^{dtg} mice were epicutaneously sensitized with EtOH+OVA or MC903+OVA (n = 3-4 per group) for 14 days. Following sensitization, free blood plasma IgE **(B)** and blood basophil surface IgE levels **(C)** were quantified. **(D)** huIgE/huFcεRIα^{dtg} mice were epicutaneously sensitized with MC903+OVA (n = 5 per group) for 14 days. On day 12 (T_{d12}), prior to treatment, free blood plasma IgE **(E)** and blood basophil surface IgE levels **(F)** were assessed for each treatment group. **(G)** huIgE/huFcεRIα^{dtg} mice were epicutaneously sensitized with MC903+OVA for 14 days, prior to treatment with 5 µM KIH_E07_79, omalizumab or PBS. Mice were sacrificed 9 hours post treatment on day 15 (T_{d15}) and free blood plasma IgE **(H)** as well as cell surface IgE levels on blood basophils **(I)**, peritoneal cavity (PEC) mast cells **(J)**, lung basophils **(K)**, ear skin basophils **(L)** and back skin mast cells **(M)** was quantified. Statistical significance was calculated by one-way ANOVA followed by Dunnett's multiple comparison post hoc test. Data is shown as individual datapoints and mean ± SEM. $*p < 0.05$, $**p < 0.01$, $***p < 0.001$, ns: not significant.

Figure 5. KIH_E07_79 interrupts anaphylaxis in mice and in human cells. (A) BMMC^{tg} were sensitized with JW8-IgE, challenged with NIP(24)BSA and treated with KIH_E07_79 or omalizumab 5 minutes post-challenge (in technical duplicates). Activation was assessed after 25 minutes ($CD107a^+$). **(B)** hFcεRIα^{tg} mice (n = 5-8 per group) were sensitized with JW8-IgE,

challenged with NIP(20)BSA, and treated 5 minutes post-challenge with PBS, KIH_E07_79 or omalizumab. Core body temperature of mice is shown as delta (Δ) temperature, with the area under the temperature curves (inset). **(C)** Isolated primary human basophils from allergic donors (n = 3) were stimulated with grass-mix allergen and treated 5 **(D)** or 25 minutes **(E)** post-challenge with PBS, KIH_E07_79 or omalizumab. Surface CD63 and LTC4 in the cell supernatants were measured 50 minutes post-challenge. **(F)** Whole blood from allergic donors (n = 3) was incubated with **(G)** or without **(H)** grass-mix allergen and treated with KIH_E07_79 after 5 minutes. Stimulation with an anti-FcεRIα antibody is shown as control. Surface CD63 was measured 25 minutes post-challenge. **(I)** Whole blood from allergic donors (n = 3) was stimulated with grass-mix allergen and treated with KIH_E07_79 at various time points post-challenge. Grass-mix allergen only and an anti-FcεRIα antibody treatment controls are shown. Surface CD63 was measured 25 minutes post-challenge **(J)**. **(K)** Isolated primary human basophils from allergic donors (n = 3) were stimulated with a predetermined EC_{opt} of grass-mix allergen and treated either 5 or 25 minutes post allergen challenge with PBS or KIH_E07_79 or omalizumab. Interleukin-13 (IL-13) in supernatants was measured 18 hours post-challenge. Significance was calculated by two-way ANOVA followed by Dunnett's multiple comparison post hoc test or by one-way ANOVA followed by Tukey's multiple comparison post hoc test. Data is shown as individual datapoints and mean ± SEM. *$p < 0.05$, **$p < 0.01$, ***$p < 0.001$, ns: not significant.

Journal Pre-proof

Figure 1

Journal Pre-proof

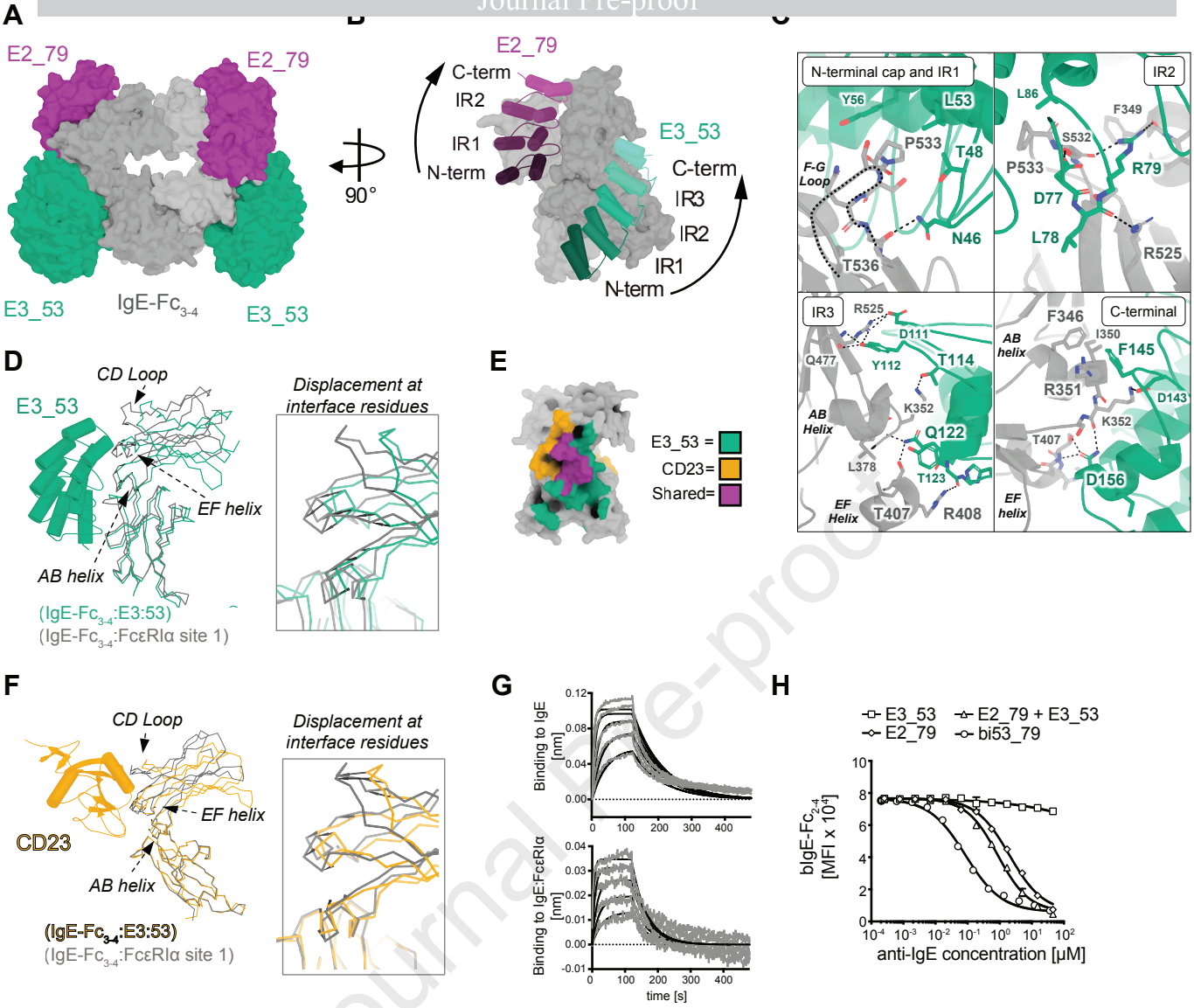
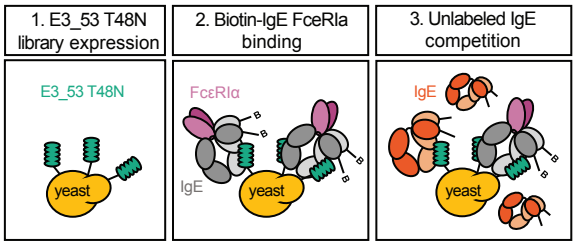


Figure 2

Journal Pre-proof

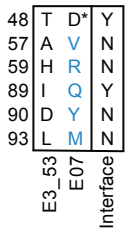
A



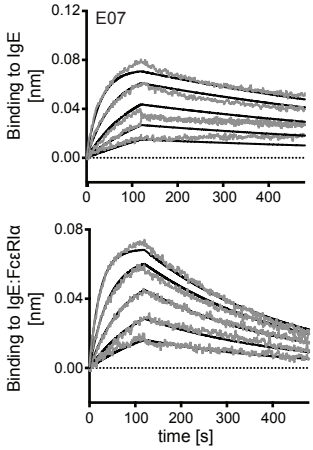
Round	Selection	bIgE [nM]	FcεRIα [nM]	IgE [nM]	Time [h]
R1	MACS	0.5	1	1	1
R2	MACS	0.5	1	1	1
R3	MACS	0.5	1	1	2
R4	MACS	0.5	1	5	2
R5	FACS	0.5	1	5	2
R1*	FACS	0.5	1	5	4

* R1 (R5 StEP Library)

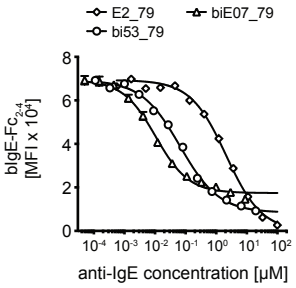
B



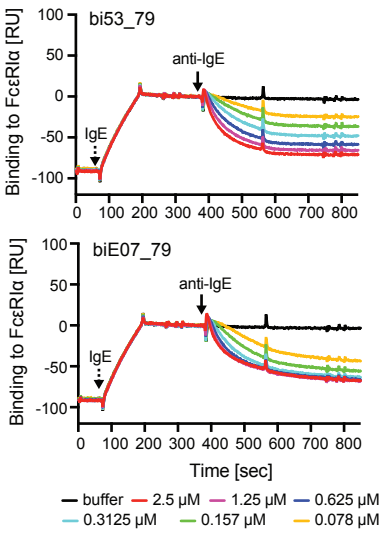
C



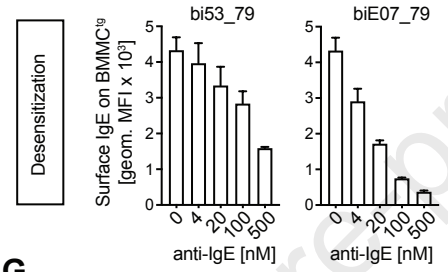
D



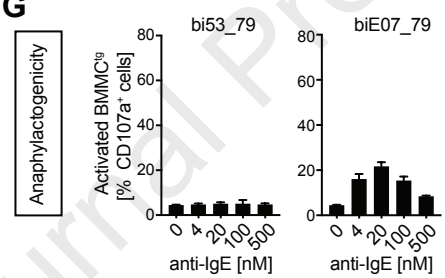
E



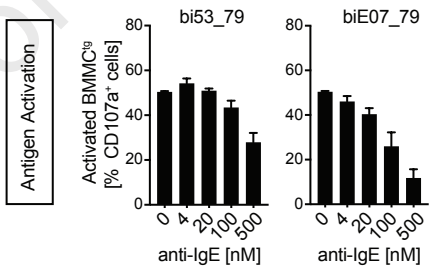
F



G



H



Journal Pre-proof

Figure 3

Journal Pre-proof

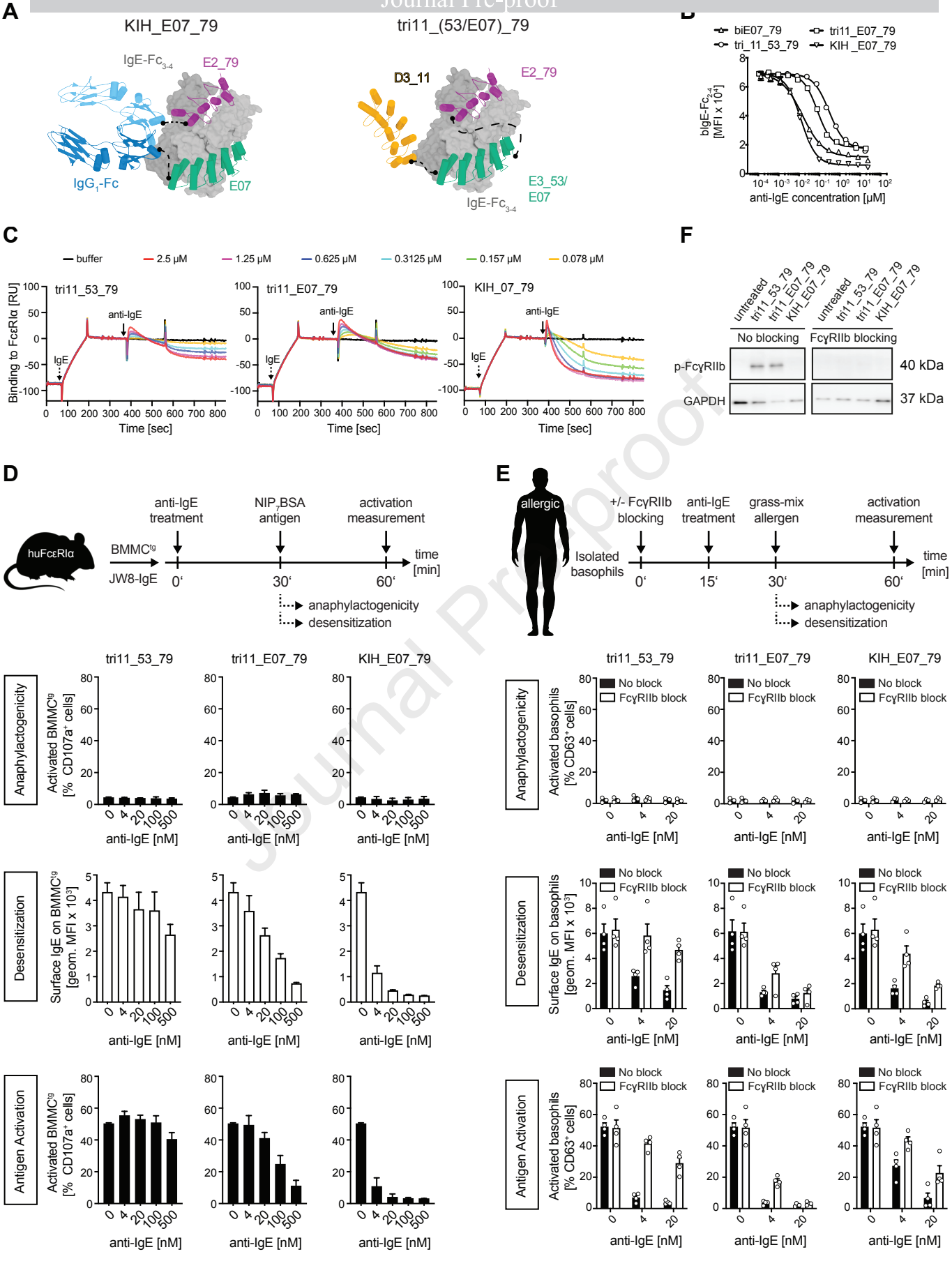


Figure 4

Journal Pre-proof

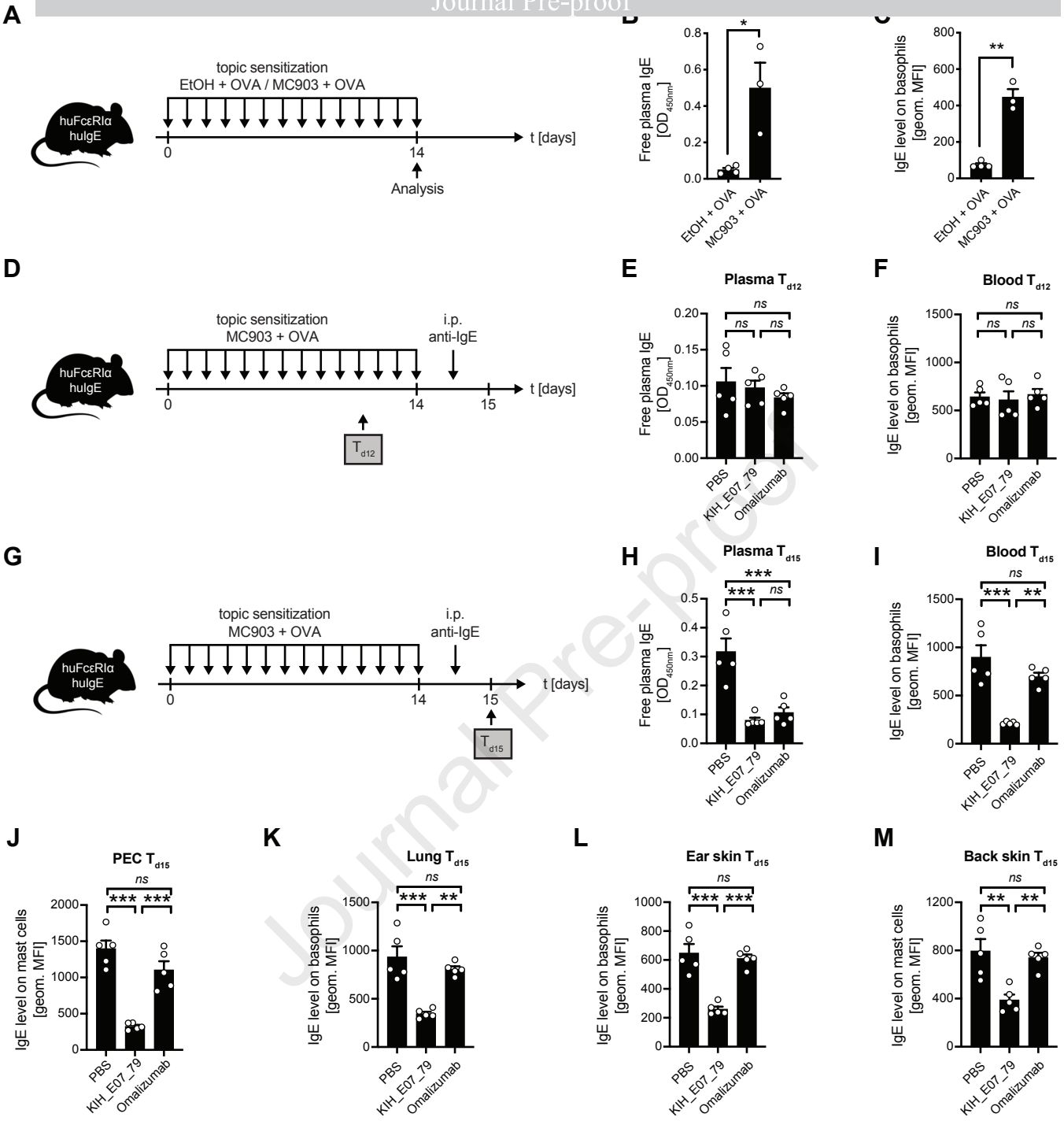


Figure 5

Journal Pre-proof

